A Network-Constrained Hydrothermal Unit Commitment Model in the Day-Ahead Electricity Market

Uriel I. Lezama-Lope
Independent Researcher
Cuernavaca, Mexico
urieliram@yahoo.com

Roger Z. Ríos-Mercado
Universidad Autónoma de Nuevo León
Graduate Program in Electrical Engineering
San Nicolás de los Garza, NL, Mexico
roger@yalma.fime.uanl.mx

José L. Ceciliano-Meza
Tecnológico de Monterrey
Campus Hermosillo
School of Engineering and Sciences
Hermosillo, Mexico
joseluis.ceciliano@tec.mx

Miguel Cecenas-Falcon
Instituto Nacional de Electricidad y Energias Limpias (INEEL)
Cuernavaca, Mexico
mcf@ineel.mx

November 2024, Revised July 2025

Abstract

The day-ahead electricity market is crucial for improving energy generation and sales planning. This paper evaluates a hydro-thermal network-constrained unit commitment model, and its solution method developed for the Mexican electricity market. The objective function maximizes the economic surplus for market participants. The problem is formulated as a mixed-integer non-linear programming problem, considering real-world constraints and a non-linear hydropower generator function. A decomposition approach is employed to solve the problem. Additionally, a new component has been introduced to handle the non-linear aspects of the hydropower generator function using a first-order Taylor's approximation. Empirical results are presented, including the solution of a representative case from Mexico's electricity market, illustrating its practical application. This novel method can be valuable in markets with substantial hydropower resources, improving the accuracy and timeliness of system operation scheduling.

Keywords: Unit commitment problem; Day-ahead electricity market; Short-term hydro scheduling; Hydropower function; Mixed-integer linear programming.

1 Introduction

In this paper, we address the Unit Commitment Problem (UCP) for the day-ahead market (DAM) in Mexico that uses the sales offers and purchase bids of the participants (generators and loads) in the market. Besides, it incorporates other constraints such as transmission losses, power flow limits in tie-lines, five simultaneous reserves with different timing, and technical features of hydraulic generators such as the Hydropower Function (HPF). Moreover, the objective function determines the maximum economic surplus of the participants. A mixed-integer non-linear programming model (MINLP) is proposed for solving this problem. A first contribution of this work is introducing a highly detailed UCP model that includes hydrothermal coordination in an electricity market.

To solve the problem, some simplifications are made to the model to reduce it into a mixed-integer linear program (MILP). A cut generation strategy embedded into a decomposition method is used for solving this model; this strategy entails decomposing the problem into a master problem (MP) and a series of non-linear sub-problems (SP). The non-linearity comes from the HPF. This function calculates the generation depending on the head of the reservoir and the water flow in the turbine. To handle this, we use a linear Taylor's approximation. This decomposition solution scheme is the main contribution of this work.

Although the Taylor's polynomial approximation has been used for energy planning (Castillo et al., 2016; Šepetanc and Pandžić, 2020; Pan et al., 2022), it has yet to be employed to approximate HPF's non-linear features. One of the advantages of this proposed linearization is its ease of implementation as compared with other traditional techniques. For instance, a common practice is to model the relationship between water discharge, generated power, and the multi-head of the reservoir of hydraulic generation as a piecewise linear function, as proposed by Diniz and Maceira (2008). However, an issue observed with the traditional piecewise linear function is its precision and sophisticated implementation. Another method is the McCormick Envelope convexification technique (Castro, 2015; Bynum et al., 2018). This technique requires the introduction of additional integer variables that make the model larger and more difficult to solve.

Several tests were conducted to show that the proposed model is consistent and applicable to markets requiring hydrothermal coordination. First, a case study from the Mexican electricity system is presented by Mexico's Independent System Operator (ISO) public information. The results indicate a consistent behavior between energy prices and demand, a suitable estimate of losses, and a satisfactory hydraulic balance. Second, we report detailed results with 320 instances built from Mexico's ISO public information; the objective is to measure mainly profits and solution times.

The remaining sections of this paper are organized as follows: Section 2 presents a survey of the main works in UCP models focused on electricity markets and hydro-thermal coordination. Section 3 shows the non-linear constraints in the DAM's mathematical model studied in this paper. The whole model can be found in the supplementary material part A. Section 4 details the solution method proposed in this work. The application of the proposed methodology is put forward in Section 5. Finally, in section 6, the conclusions and possible extensions are discussed.

2 Related work

The literature on unit commitment models can be roughly classified into deterministic and stochastic models. Since our paper deals with a deterministic model, in this section, we focus our literature discussion in deterministic approaches. However, research on stochastic models has been very active in the past few years, including works on modeling improvement (Polimeni et al., 2023), decomposition methods (Colonetti and Finardi, 2020; Guo et al., 2024; Lima et al., 2024), scenario reduction-based methods (Kwon and Kim, 2020), and statistical methods (Olivos and Valenzuela, 2025) for stochastic programming, multi-objective optimization (Mena et al., 2023), robust optimization (Shang et al., 2024), and machine learning (Liu et al., 2023) approaches. The reader is referred to the work by Håberg (2019), who provide an excellent survey on stochastic unit commitment models prior to 2020.

With the rise of competitive electricity markets, UCP models have changed from minimizing production costs to maximizing profits or social welfare (Abdi, 2021); the new markets model includes the previous UCP constraints but adds new variants to meet new economic regulations. Bisanovic et al. (2010) present a market UCP model in high detail, although the paper focuses on handling long-term bilateral contracts. However, it was tested on a small electrical system. Chow et al. (2005) present the optimization model for energy and ancillary service in New York ISO. This model includes different types of reserves. Ma et al. (2009) present the network-constrained unit commitment and dispatch model implemented for Midwest ISO's DAM; it optimizes both energy and ancillary services. In these previous market models, hydrothermal coordination is not included. Regulation is not included in these models either.

Hydrothermal coordination is essential because it impacts future costs, secure operation, and security in reservoirs and rivers. Babona and Rossell Pujós (1999) introduce an uncoupled formulation of hydrothermal coordination and solve it with a MILP solver. However, the model lacks other significant operational constraints for effective real-life operation.

Unlike the previous model, Yu et al. (2000) include several operational and hydro constraints such as losses, hydro production, water storage balance, water storage limits, water discharge limits, the relationship between water head and water storage, and import/export limits. The model solves the MIP-based hydrothermal coordination using off-the-shelf solvers. Conejo et al. (2002) introduce a MIP-based formulation that links hydropower production, water discharge, and water head. This model enables self-scheduling for hydro-generating companies in the day-ahead power pool electricity market, incorporating the hydro component. The authors employ discretized curves per unit to capture the nonlinear relationship between the reservoir head, hydro unit power output, and water discharge, selecting a specific curve based on reservoir volume. However, the model overlooks water travel time delays between upstream and downstream reservoirs, assuming one-hour delays. It also lacks thermal unit commitment. For a study considering water travel time delays, refer to Gil et al. (2003). Catalão et al. (2010) addressed these issues by proposing a mixed-integer quadratic programming model for scheduling pure cascaded hydro systems. While this model does not account for water travel time delays, it offers several advantages. It incorporates head dependency, prohibited operating zones (POZ), and discharging ramping constraints. Furthermore, it integrates the effect of changes in the head into a single function for water discharge and storage, eliminating the need for multiple curves for different heads, as previously seen in Conejo et al. (2002). This simplification reduces the computational load for solving hydro generation scheduling. Catalão et al. (2010) also provided test models, including examples with three and seven cascaded reservoirs.

Bisanovic et al. (2008) present a comprehensive model for hydro and thermal generators within a DAM. This model handles a multi-reservoir hydro system with hydraulic coupling, discharge limits, spillage, and reservoir level constraints. It uses a piecewise linear function, approximating the nonlinear power-discharge function. However, it overlooks water travel time delays and simplifies the water head-to-volume relationship with a piecewise linear function, resulting in underestimating hydropower production.

Various intricate factors are considered in Santos et al.'s real-world model with 162 cascaded reservoirs (Santos et al., 2020) for day-ahead generation scheduling in Brazil. These include reservoir limits, discharge and spilled outflows, competing water uses, evaporation, water delay times, pumping stations, and re-pumping to other reservoirs. Hydro generation is represented by a concave piecewise linear function with coefficients tied to reservoir storage, turbines, and spilled outflows. While Santos does not delve into the specifics of the HPF model, it is based on a detailed model by Diniz and Souza (2014). Furthermore, Santos' model meticulously incorporates thermal generation constraints. This comprehensive model closely mirrors real-life scenarios. The authors devised an iterative procedure utilizing an interior point method and branch and cut, employing the CPLEX solver to solve it.

Álvarez López et al. (2012) researched electricity planning in Mexico, introducing a Mixed Integer Quadratically Constrained Program (MICQP) for UCP with considerable detail focusing on fuel management. In a follow-up paper, Álvarez López et al. (2015) introduced a MILP for UCP, including constraints for modeling regulation, spinning, and non-spinning reserves. Those works are antecedents to many aspects of the proposed model that include hydro constraints in the new open electricity market, thus making it more in line with the system's current needs for Mexico.

Bisanovic et al. (2010), Chow et al. (2005), Ma et al. (2009) outline thermal UCP models in some electricity markets in the United States that optimizes energy and reserves similar to the DAM in Mexico. However, those works do not include hydrothermal coordination. Specialized works on hydro generation are due to Babona and Rossell Pujós (1999), Yu et al. (2000), Gil et al. (2003), and Catalão et al. (2010). They employ different methods to model the non-linear relationship between the reservoir head, water discharge, and generation. Conejo et al. (2002), and Bisanovic et al. (2008) outline models that include the hydrothermal coordination component in a DAM. However, their hydraulic modeling can be improved to attain results with more accuracy and less computational work. Santos et al. (2020) elaborated a full-fledged model for day-ahead scheduling in Brazil. However, the calculation of transmission losses is not explicit, and different types of ancillary services are omitted. Furthermore, the POZ are not considered either. These aspects are essential to obtain a better schedule. Table 1 highlights the research work that influences our research the most. For more detailed reviews, we refer to the work of Kong et al. (2020) who present an overview on models and solution algorithms for the unit-based short-term hydro scheduling problem, the work by Taktak and D'Ambrosio (2016) who present an overview on mathematical optimization approaches for the deterministic UCP in hydro valleys, and the work by de Queiroz (2016) who presents a survey on models and methods for stochastic hydro-thermal scheduling. Moreover, the short-term scheduling is not conducted by itself, it relies on water values (or alternative costs) pricing hydro-resources. The overview of hydropower toolchains by Helseth et al. (2023) provide relevant background for the readers.

Our work presents a highly detailed hydro-thermal MINLP model that considers the main elements outlined in the cited articles. This model is a reduced version of the DAM model published by Mexico ISO (Ceciliano-Meza et al., 2016), which schedules generators in the electricity market by combining loss estimation, network constraint, and HPF non-linearity. However, that document does not provide details about the solution method, making our work relevant as it presents a concise approach to solving this DAM model. Additionally, while the document published by ISO Mexico only models the energy limitation of power plants associated with a reservoir, our work takes a more comprehensive approach by considering the volume balance per reservoir, coupling between cascading reservoirs, water travel time, and spillage. Finally, we address the undocumented aspect of how the HPF constraint is handled in the Mexico ISO document, which is an important consideration. In summary, our paper presents a general method for incorporating non-linear HPF constraints, transmission loss constraints that approximate linearity, and network flow constraints into the scheduling of generators in the day-ahead market.

The main innovation of this work consists of applying Taylor's polynomial approximation embedded in a decomposition method to tackle the non-linear hydropower function and not a piecewise function. The linear approximation is calculated while the method runs.

Table 1: Research work comparison.

	Methodology and Features	Advantages and Disadvantages
Babona and Rossell Pujós (1999)	Developed a MILP solver for hydrothermal coordination	Includes spinning reserves and network constraints. Lacks some operational constraints.
Yu et al. (2000)	Presented a MIP-based hydrothermal coordination model	Considers both operational and hydro constraints. Oversimplified water travel time delays.
Conejo et al. (2002)	Created an MIP-based hydropower production model for self-scheduling in a DAM with hydro	Considers hydro constraints and scheduling. Does not account for water travel time delays.
Catalão et al. (2010)	Developed an MIQP model for scheduling pure cascaded hydro units	Includes head dependency and operating restricted zones.
Bisanovic et al. (2010)	Outlined thermal UCP models for energy and reserves optimization	Optimized energy and reserves for thermal units. No hydrothermal coordination.
Álvarez López et al. (2015)	Introduced MICQP and MILP for UCP with a focus on fuel management, including regulation, spinning, and non-spinning reserves	Detailed UCP model with a fuel management focus. Lack of hydro constraints, not fully adapted to Mexico's current electricity market needs.
Santos et al. (2020)	Presented a real-world model for day-ahead scheduling in Brazil, focusing on hydro generation and thermal constraints. Use a piecewise function for HPF.	Comprehensive, real-life model that reproduces practical scenarios. Lack of explicit details on transmission losses, ancillary services, and POZ.
Our work	Highly detailed hydro and thermal MINLP model based on ISO Mexico's DAM model, addressing HPF constraints. Use a Taylor series polynomial approximation for HPF.	A detailed approach covering HPF handling, transmission loss constraints, ISO Mexico DAM model, and a comprehensive hydrothermal mode.

3 Mathematical formulation

The proposed integer programming model is fully described in Chapter 5 of the doctoral thesis of Lezama Lope (2023). In addition, we provide the reader with a supplementary accompanying document. Both, the thesis and the document, are available at the following URL:
http://yalma.fime.uanl.mx/~roger/ftp/Submitted_JCAES.

The supplementary material part A presents in detail the integer programming model used to solve the DAM. The model focuses on minimizing all operation costs subject to power balance, loads, reserve, generation limits, ramps, up/down times, variable start-ups, hydraulic, hydropower function (HPF), network flow, transmission losses, and logical constraints. Due to space limitations, in this paper we present the nonlinear HPF constraints, transmission loss constraints that approximate linearity, and the power flow limit constraints.

3.1 Notation

Sets and indices

$\mathcal{BR}$ Set of electric tie-lines; $br \in \mathcal{BR}$

$\mathcal{E}$ Set of reservoirs; $e \in \mathcal{E}$

$\mathcal{G}^{\mathrm{HI}}$ Set of hydroelectric generators; $g \in \mathcal{G}^{\mathrm{HI}}$

$\mathcal{G}^{\mathrm{TE}}$ Set of thermal generators; $g \in \mathcal{G}^{\mathrm{TE}}$

$\mathcal{HI}_e$ Set of hydro generators located in reservoir; $e \in \mathcal{E}$; $g \in \mathcal{HI}_e$

$\mathcal{HI}_\nu$ Set of hydro generators that discharge water over a river

$\mathcal{N}$ Set for electric nodes in the system; $n \in \mathcal{N}$ $\nu \in \mathcal{V}_e^{\mathrm{d}}$; $g \in \mathcal{HI}_v$

$\mathcal{T}$ Set of periods in the planning horizon; $t \in \mathcal{T}$

$\mathcal{V}_e^{\mathrm{c}}$ Set of rivers converging to reservoir; $e \in \mathcal{E}$; $\nu \in \mathcal{V}_e^{\mathrm{c}}$

$\mathcal{V}_e^{\mathrm{d}}$ Set of rivers diverging from reservoir; $e \in \mathcal{E}$; $\nu \in \mathcal{V}_e^{\mathrm{d}}$

Parameters

$a_{1,g}, a_{2,g}, a_{3,g}$ Constant coefficients in the HPF (1) for $g \in \mathcal{G}^{\mathrm{HI}}$; with units in MW, MW·s/m^3, and MW·s^2/m^6, respectively.

$b_{1,g}, b_{2,g}, b_{3,g}$ Linear coefficients associated with the water head h in the HPF (1) for $g \in \mathcal{G}^{\mathrm{HI}}$; with units in MW/m, MW·s/m^4, and MW·s^2/m^7, respectively.

$c_{1,g}, c_{2,g}, c_{3,g}$ Quadratic coefficients associated with the squared water head h^2 in the HPF (1) for $g \in \mathcal{G}^{\mathrm{HI}}$; with units in MW/m^2, MW·s/m^5, and MW·s^2/m^8, respectively.

$\overline{fn}_{br,t}$,$\overline{fp}_{br,t}$ Maximum value for the power counterflow and flow on tie-line $br \in \mathcal{BR}$ in period $t \in \mathcal{T}$, respectively; in MW.

$LSF_{n,t}$ Sensitivity transmission losses in node $n \in \mathcal{N}$ with regard to changes in power injections in node $n \in \mathcal{N}$ in period $t \in \mathcal{T}$; dimensionless

$PTDF_{br,n,t}$ power transfer distribution factors in $br \in \mathcal{BR}$ at a node $n \in \mathcal{N}$.

R_{br} Electric resistance of a tie-line $br \in \mathcal{BR}$; dimensionless

Decision variables

$f_{br,t}$ Power flow on br in period $t \in \mathcal{T}$; in MW

$h_{v,t}$ Net hydraulic head of a river ν in period $t \in \mathcal{T}$; in m

$iny_{n,t}$ Amount of power input at node $n \in \mathcal{N}$ in period $t \in \mathcal{T}$, in MW

$Loss_t^{SP}$ Amount of exact transmission losses in period $t \in \mathcal{T}$, in MW

$Loss_t^{MP}$ Amount of approximate transmission losses in period $t \in \mathcal{T}$, in MW

$p_{g,t}$ Amount of power a generator $g \in \mathcal{G}^{\mathrm{TE}} \cup \mathcal{G}^{\mathrm{HI}}$ produces in period $t \in \mathcal{T}$, in MW

$q_{g,t}$ Water discharge of generator g in period $t \in \mathcal{T}$; in m^3/s

$u_{g,t}$ Equal to 1 if generator $g \in \mathcal{G}^{\mathrm{TE}} \cup \mathcal{G}^{\mathrm{HI}}$ is online in period $t \in \mathcal{T}$, and 0 otherwise

$\omega_{e,t}$ Water volume in reservoir e in period $t \in \mathcal{T}$; in m^3

3.2 Hydraulic generation

Hydro generation power depends on the turbine water discharge rate and the reservoir head, both quadratically. The function used here is known as Glimn-Kirchmayer (Kotharij and Dhillon, 2010). It is given by;

$$\begin{aligned} p_{g,t} =& u_{g,t}\big((a_{1,g} + b_{1,g}h_{\nu,t} + c_{1,g}h^2_{\nu,t}) + (a_{2,g} + b_{2,g}h_{\nu,t} + c_{2,g}h^2_{\nu,t})q_{g,t} \\ &+ (a_{3,g} + b_{3,g}h_{\nu,t} + c_{3,g}h^2_{\nu,t})q^2_{g,t}\big), \qquad g \in \mathcal{HI}_\nu,\ \nu \in \mathcal{V}^{\mathrm{d}}_e,\ e \in \mathcal{E},\ t \in \mathcal{T}. \end{aligned} \tag{1}$$

This is known as the HPF, and its parameters $\{a_{1,g}, ..., c_{3,g}\}$ depend on the reservoir design, turbine, and generator features.

The nonlinear HPF constraints require an approximation method for smooth integration into a MILP. In our work, we utilize the Taylor polynomial approximation method, which produces an alternative constraint to replace (1). Although a second-order approximation of (1) would undoubtedly offer improved accuracy, we deliberately employ a first-order linearization to ensure compatibility with the MILP formulation. This choice strikes a practical balance between model fidelity and tractability, as second-order terms introduce nonlinearities that MILP solvers cannot directly handle. Moreover, given the iterative nature of the solution process, such a level of precision is not required at this stage.

3.3 Power flow limits

The power flow in a transmission tie-line is modeled as follows:

$$f_{br,t} = \sum_{n \in \mathcal{N}} PTDF_{br,n,t} iny_{n,t}, \qquad br \in \mathcal{BR},\ t \in \mathcal{T}, \tag{2}$$

where $f_{br,t}$ represents the power flow in a transmission tie-line br which depends on parameters $PTDF_{br,n,t}$ and the power injection $iny_{n,t}$ for each bus n for each period t. The variable $iny_{n,t}$ is a key decision variable that represents the net injection at bus n and time t, computed as the total generation minus the demand at that bus. A detailed description of the PTDF's calculation is explained by Hinojosa and Gutiérrez-Alcaraz (2017). Also, the following constraints fix the maximum flow and counterflow power limits in tie-line br.

$$\overline{fn}_{br,t} \leq f_{br,t} \leq \overline{fp}_{br,t}, \qquad t \in \mathcal{T}. \tag{3}$$

Although constraints (2) and (3) capture the relationship between bus injections and line flows, along with the operational limits of each tie-line, they are omitted from the initial formulation to improve computational efficiency. They are instead added iteratively during the solution process when violations are detected, yielding a more compact and tractable problem.

3.4 Transmission losses

The losses in the system are calculated using the following constraints. The non-linear feature of these constraints requires an approximation method to be successfully integrated into a MILP. The method used in our work is tangent planes and provides a set of alternative constraints to replace these constraints.

$$Loss_t = \sum_{br \in \mathcal{BR}} R_{br}(f_{br,t})^2, \qquad t \in \mathcal{T}. \tag{4}$$

4 Solution method

The model posed in Section 3 has continuous and binary variables and some non-linear components such as the HPF (1) and the transmission losses (4). It also incorporates power flow constraints in the network. Those constraints keep the power flow within safe limits. In typical real-world instances, with 7000+ buses, 8000+ lines, and 400+ generators, simultaneously including all transmission constraints can significantly increase solution times. Consequently, due to this complexity, a common solution strategy involves initially relaxing constraints (4) and subsequently incorporating them into the model as violations are detected (Ezzati et al., 2010).

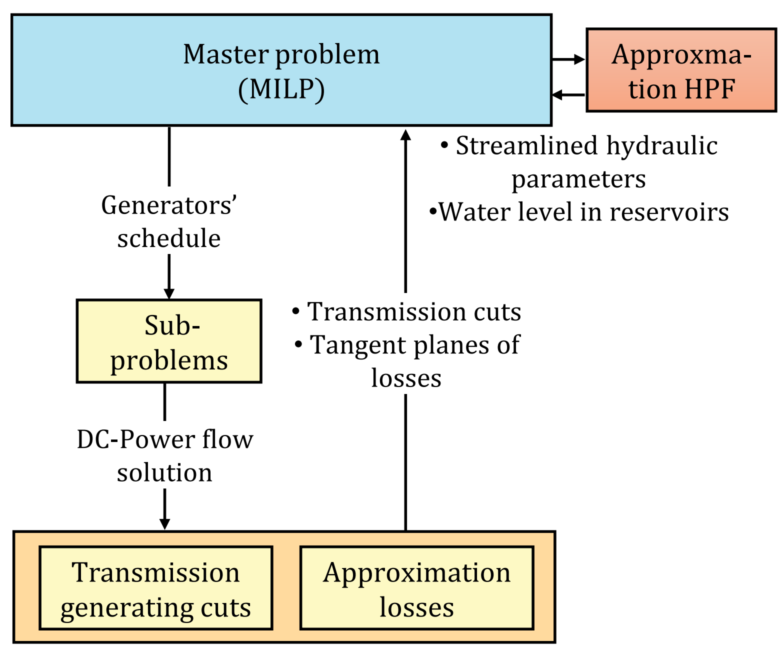

Figure 1: Iterative decomposition method, based on García Félix (2017).

The iterative approach depicted in Figure 1 involves solving a master problem (MP) that initially disregards transmission constraints and loss estimation. The resulting generator schedule is used to identify overloaded transmission tie-lines and calculate losses in 24 power flow sub-problems. The information obtained from these sub-problems is then used to generate new constraints, such as transmission cuts and tangent planes of losses. The linearized HPF function is also updated. All the new constraints are added to the master problem, which is then solved again. This process is repeated until no further transmission violations occur and the criterion for losses is satisfied.

The MP is formed by the objective function (S1) and the set of constraints (S2)-(S39), (S41)-(S42), (S44)-(S52), contained all in the supplementary material, part A. Note that the linear constraints (7) replace the HPF non-linear constraints (1) so this can be handled as a MILP. Similarly, constraints (5) replace constraints (4). The MP is solved to determine the generators' schedule, i.e., the MP aims to determine the generators to be turned on/off and their corresponding power production levels.

The status of generators is fixed and sent to the SP, which calculates the power flow in the lines using the DC Power Flow method. With those results, a feasibility test can identify possible violations of network constraints (3). These violations or cuts are added to the model and passed to the MP. Moreover, constraints (2) that represent the power flow in the violated tie-lines are added too. Marín-Cano et al. (2019) and dos Santos and Diniz (2011) provide some examples of these approaches, including user cut adding iteratively.

Constraints (4) consider the losses in the system. However, they are non-linear and cannot be added directly to a linear master problem. Therefore, the Tangential Approximation Method developed by Geoffrion (1970) is used to tackle its non-linearity. Notably, its application in the market in Mexico is widely documented by García Félix (2017). The constraints (tangential planes) have the following mathematical structure:

$$Loss_t - \sum_{n \in \mathcal{N}} LSF_{n,t}^{k-1} iny_{n,t} \geq Loss_t^{SP} - \sum_{n \in \mathcal{N}} LSF_{n,t}^{k-1} iny_{n,t}^{k-1}, \qquad t \in \mathcal{T}. \tag{5}$$

The tangential plane method replaces the constraint of losses specified in (4) in the MILP model by incorporating linear constraints with the same structure as in (5). The approximation can be improved by iteratively adding more tangents (4). This method is an exact approach that can find a globally optimal solution with a certain level of accuracy by creating a concave problem equivalent to the original problem, provided that the nonlinear constraints being approximated complies with convexity, compactness, and continuity assumptions, as proposed by Geoffrion (1970). The accuracy of the solution can be measured by comparing the losses estimated by the MILP method with those calculated using the DC power flow method for subproblems.

The variable $Loss_t^{SP}$ determines the exact losses in the network obtained from substituting the power flow in (4). However, unlike the variable $Loss_t^{SP}$, $Loss_t$ is a variable in the MP that approximates the total transmission loss in the system. The loss sensitivity factors parameters $LSF_{n,t}^{k-1}$ represent the variation in losses in the system when modifying a power unit in each node.

The parameters $LSF_{n,t}^{k-1}$ are calculated at the end of each iteration k and are expressed in the following equation:

$$LSF_{n,t}^{k-1} = \frac{\partial Loss_t}{\partial iny_{n,t}}\Big|_{iny_{n,t}=iny_{n,t}^{k-1}}, \qquad n \in \mathcal{N},\ t \in \mathcal{T},\ k \geq 1. \tag{6}$$

Equation (6) is solved numerically, and parameters $LSF_{n,t}^{k-1}$ are used to build a new set of constraints (5) (Menezes and da Suva, 2006).

A decomposition approach such as the one presented in this paper is widely used to plan the operation of real-life power systems. However, this work has added a new component to deal with HPF's non-linear characteristics using the first-order Taylor polynomial approximation. The method provides the following constraints that replace (1) in the MP. The procedure for obtaining this constraint and its parameters $QW_{g,e,t}, Q_{g,e,t}, W_{g,e,t}$, involves a new application of the Glimn-Kirchmayer model, which maps reservoir level to volume to fit available field data.

$$g_{g,t} \leq \beta_{g,t} QW_{g,e,t} + Q_{g,e,t} q_{g,t} + W_{g,e,t} w_{e,t}, \qquad g \in \mathcal{HI}_e,\ e \in \mathcal{E},\ t \in \mathcal{T} \tag{7}$$

Finally, in each iteration k of the algorithm, the water levels in reservoirs are updated, and the streamlining of constraint parameters (7) is also carried out.

Description of algorithm

The proposed method in this work is outlined in Algorithm 1. This algorithm begins by solving the MP using CPLEX. In the first iteration, the MP does not include transmission losses (tangential planes) nor any transmission constraints (cuts). The solution is saved in X, which contains the value of all the decision variables of the MP. An iterative process begins and runs until the stopping criteria are met. There are two conditions for stopping. The first is when the relative error in approximation losses ($ErrLosses$) is greater or equal to the given tolerance ($tolerance$). The second one is the absence of violations of the safe transmission limits. Within the loop, the method `SolvingSP()` that consists of solving a series of SPs using the DC Power Flow method is run, one for each period t. Then, power flow in the lines (F) is calculated using the injection values at each node and the network's topology, based on the SP's results. Then, `GeneratingCuts()` identifies violations of safe operational limits in any branch. Whenever constraint (2) (the linearized power flow equation) is violated, a cut is generated to enforce feasibility. These cuts also incorporate constraint (3), which imposes upper and lower bounds on the flow for each branch and time period. Only constraints that are found to be violated in the SPs are added to the MP. The relevant decision variables involved in these cuts are the nodal power injections $iny_{n,t}$, while the PTDF coefficients $PTDF_{br,n,t}$ are fixed parameters that capture the network's sensitivity to nodal injections and are derived from the topology and impedance data. The cuts are added to the MP via the `AddingCuts()` procedure. Next, the exact losses are calculated using (4) and are registered in $Loss_t^{SP}$. Then `AddingTangentPlanes()` generates the tangent planes of losses with the structure (5). Subsequently, the tangent planes are added to the MP. After this, MP is solved again, considering losses and safe limits in the tie-lines. Then, the maximum relative error in the estimated losses in all periods t is calculated and registered in $ErrLosses$. The value of the variable $Loss_t$, obtained from the MP, is the sum of estimated losses by multiplying $LSF_{n,t}^{k-1}$ by injections in $y_{n,t}^{k-1}$ at each node. Finally, the parameters $LSF_{n,t}^{k}$ are updated with (6) by using the new transmission losses in the lines $Loss_k^{SP}$ and the new injections in the nodes $iny_{n,t}^{k}$. When there are no more violations in the safe limits of the transmission, and a user-defined loss tolerance is reached, the algorithm stops.

Procedure 1 Iterative method employed

Input: P:=Instance of the problem, *tolerance*
Output: X^*:=An optimal solution to the problem
$k \leftarrow 1$
$Lossi^{SP} \leftarrow 0$
$LSF^{k-1}n, i \leftarrow 0$
$Errlosses \leftarrow \infty$ {Relative difference of the losses between approximated and exact losses}
Cuts $\leftarrow \phi$ {Set of transmission cuts}
$X \leftarrow$ SolvingMP()
while ($Errlosses \geq tolerance$) or (Cuts $\neq \phi$) **do**
  Cuts $\leftarrow \phi$
  F $\leftarrow$ SolvingSP(X) {Power flow in lines}
  Cuts $\leftarrow$ GeneratingCuts(F)
  if Cuts $\neq \phi$ **then**
    MP $\leftarrow$ AddingCuts(MP,Cuts)
  end if
  $Loss^{SP}i \leftarrow$ CalculatingLosses(F)
  MP $\leftarrow$ AddingTangentPlanes(MP, $LSF^{k-1}n, i$, $Loss_i^{SP}$)
  $X \leftarrow$ SolvingMP()
  $Errlosses \leftarrow \max((Loss_i - Loss_i^{SP})/Loss_i), \forall i \in \mathcal{I}$
  $LSF^{k}n, i \leftarrow$ updatingLSF()
  $k \leftarrow k + 1$
end while
return X^*

Linearization of the hydro power function using Taylor Polynomial

The value of the effective hydraulic head $h_{\nu,t}$ in constraints (1) is calculated with the height of forebay water minus the tailwater level minus the head losses that occur due to friction in pipes as follows:

$$h_{\nu,t} = \gamma(\omega_{e,t-1}) - \mu\left(\sum_{g\in\mathcal{H}_\nu} q_{g,t}\right) - \sum_{g\in\mathcal{H}_\nu} \zeta(q_{g,t}), \qquad \nu \in \mathcal{V}_e^r,\, e \in \mathcal{E},\, t \in \mathcal{T}, \tag{8}$$

where $\gamma()$ represents a function with an input volume and an output forebay height and it is often non-linear; $\mu()$ represents a function with an input water discharge and an output tailwater level; $\zeta()$ is a function with an input water discharge and an output the head losses. These functions depend on each reservoir's design; therefore, $\gamma()$, $\mu()$, and $\zeta()$ are written generically.

The method to linearize the hydropower function begins by transforming (1) in a function that depends on the flow $q_{g,t}$ and the volume $\omega_{e,t}$ as follows:

$$\begin{aligned} g_{g,t} =& \beta_{g,t}\big((A_{1,g} + B_{1,g}\omega_{e,t} + C_{1,g}\omega_{e,t}^2) + (A_{2,g} + B_{2,g}\omega_{e,t} + C_{2,g}\omega_{e,t}^2)q_{g,t} \\ &+ (A_{3,g} + B_{3,g}\omega_{e,t} + C_{3,g}\omega_{e,t}^2)q_{g,t}^2\big), \qquad g \in \mathcal{HI}_\nu,\, \nu \in \mathcal{V}_e^{\mathrm{d}},\, e \in \mathcal{E},\, t \in \mathcal{T} \end{aligned} \tag{9}$$

Then, parameters $\{A_{1,g}, ..., C_{3,g}\}$ of (9) can be calculated from parameters $\{a_{1,g}, ..., c_{3,g}\}$ of (1). An equivalent approximation between both constraints is shown in the following set of equations:

$$A_{i,g} = a_{i,g}, \qquad g \in \mathcal{HI}_\nu,\, i = 1,2,3 \tag{10}$$

$$B_{i,g} \approx \frac{b_{i,g}h_{\nu,t}^*}{\omega_{e,t}^*}, \qquad g \in \mathcal{HI}_\nu,\, \nu \in \mathcal{V}_e^{\mathrm{d}},\, e \in \mathcal{E},\, t \in \mathcal{T},\, i = 1,2,3 \tag{11}$$

$$C_{i,g} \approx \frac{c_{i,g}(h_{\nu,t}^*)^2}{(\omega_{e,t}^*)^2}, \qquad g \in \mathcal{HI}_\nu,\, \nu \in \mathcal{V}_e^{\mathrm{d}},\, e \in \mathcal{E},\, t \in \mathcal{T},\, i = 1,2,3 \tag{12}$$

Parameter $\omega_{e,t}^*$ is the water volume obtained by the master problem (MP) in each iteration. The non-linear function (8) is used to obtain the effective head height $h_{\nu,t}^*$.

Now, by substituting (10)–(12) into (9), we obtain the following equation:

$$\begin{aligned} g_{g,t} =& \beta_{g,t}\Big((a_{1,g} + \frac{b_{1,g}h_{\nu,t}^*}{\omega_{e,t}^*}\omega_{e,t} + \frac{c_{1,g}(h_{\nu,t}^*)^2}{(\omega_{e,t}^*)^2}\omega_{e,t}^2) + (a_{2,g} + \frac{b_{2,g}h_{\nu,t}^*}{\omega_{e,t}^*}\omega_{e,t}\omega_{e,t} + \frac{c_{2,g}(h_{\nu,t}^*)^2}{(\omega_{e,t}^*)^2}\omega_{e,t}^2)q_{g,t} \\ &+ (a_{3,g} + \frac{b_{3,g}h_{\nu,t}^*}{\omega_{e,t}^*}\omega_{e,t} + \frac{c_{3,g}(h_{\nu,t}^*)^2}{(\omega_{e,t}^*)^2}\omega_{e,t}^2)q_{g,t}^2\Big), \qquad g \in \mathcal{HI}_\nu,\, \nu \in \mathcal{V}_e^{\mathrm{d}},\, e \in \mathcal{E},\, t \in \mathcal{T} \end{aligned} \tag{13}$$

Subsequently, (13) is linearized using the first-order Taylor polynomial method for two variables ($\omega_{e,t}$ and $q_{g,t}$) around the current operating conditions, denoted as $w_{e,t} = \omega_{e,t}^*$ and $q_{g,t} = q_{g,t}^*$. To achieve this, we first need to compute partial derivatives of the function with respect to both variables, $h(\omega_{e,t}, q_{g,t})$. These partial derivatives are essential for the linearization process.

The first-order Taylor polynomial approximation for two variables can be expressed as:

$$f(x, y) \approx f(a, b) + \frac{\partial f}{\partial x}(a, b)(x - a) + \frac{\partial f}{\partial y}(a, b)(y - b) \tag{14}$$

where $f(x, y)$ represents the function's value at the point of interest, (a, b) is the point about which the function is linearized, and $\frac{\partial f}{\partial x}(a, b)$ and $\frac{\partial f}{\partial y}(a, b)$ denote the partial derivatives of the function with respect to variables x and y evaluated at the same point. In our case, the function we want to approximate is (13), denoted as $g_{g,t}$. By applying the Taylor polynomial approximation method to $g_{g,t}$, we can rewrite it as:

$$g_{g,t} \approx g^*_{g,t} + \frac{\partial g_{g,t}}{\partial \omega_{e,t}}(\omega_{e,t} - \omega^*_{e,t}) + \frac{\partial g_{g,t}}{\partial q_{g,t}}(q_{g,t} - q^*_{g,t}), \qquad g \in \mathcal{HI}_\nu,\, \nu \in \mathcal{V}^{\mathrm{d}}_e,\, e \in \mathcal{E},\, t \in \mathcal{T} \tag{15}$$

where $g_{g,t}$ is the value of the function at the operating point $w^*_{e,t}$ and $q^*_{e,t}$. Linearization provides an approximation of $g_{g,t}$, simplifying modeling and aiding subsequent computations. After algebraic manipulations, we have obtain (7), where parameters $QW_{g,e,t}$, $Q_{g,e,t}$, and $W_{g,e,t}$ are found with the three equations below, respectively:

$$QW_{g,e,t} = \big(g_{g,t}(q_{g,t}, \omega_{e,t}) - Q_{g,e,t}q_{g,t} - W_{g,e,t}\omega_{e,t}\big) \qquad g \in \mathcal{HI}_e,\, e \in \mathcal{E},\, t \in \mathcal{T} \tag{16}$$

$$\begin{aligned} Q_{g,e,t} &= A_{2,g} + B_{2,g}\omega_{e,t} + C_{2,g}(\omega_{e,t})^2 \\ &\quad + 2(A_{3,g} + B_{3,g}\omega_{e,t} + C_{3,g}(\omega_{e,t})^2)q_{g,t}, \qquad g \in \mathcal{HI}_e,\, e \in \mathcal{E} \end{aligned} \tag{17}$$

$$\begin{aligned} W_{g,e,t} &= B_{1,g} + B_{2,g}q_{g,t} + B_{3,g}(q_{g,t})^2 \\ &\quad + 2(C_{1,g} + C_{2,g}q_{g,t} + C_{3,g}((q_{g,t})^2)\omega_{e,t}, \qquad g \in \mathcal{HI}_e,\, e \in \mathcal{E} \end{aligned} \tag{18}$$

The first time the MP is solved, the $\omega^*_{e,t}$ is the initial volume $\omega_{e,0}$ and $q^*_{g,t}$ is the value of the flow in the turbine at maximum efficiency according to its design features.

Finally, the water levels $\omega^*_{e,t}$ and $h^*_{\nu,t}$ are updated in each iteration k of the Algorithm described in the paper. Furthermore, the streamlining of parameters from (10)–(12) is carried out in each iteration too. It is worth mentioning that the accuracy of the Taylor's approximation depends on the number of iterations of the algorithm.

5 Experimental work

Two sets of experiments are conducted to evaluate the model's performance and the method employed in this work.

The model and method were coded with Intel Fortran and C++ languages using the Intel one API DPC++/C++ version 2020. The solver employed was 64-bit CPLEX 12.10 with an optimality gap of 0.0001, running on a 64-bit with 16GB of RAM and an Intel(R) Xeon(R) CPU E3-1240 v3 @ 3.40GHz. Unlike the original method used for the ISO for planning MEM, this work omits several infeasibilities, such as variables dealing with unbalances, load cuts, surplus, network, and hydraulic violations.

5.1 Experiment 1: A case study

This section presents a case study that outlines the model. This instance is built from data published by CENACE in Mexico using the limits and offers of generators found in https://www.

cenace.gob.mx/Paginas/SIM/Reportes/OfertasMDA.aspx. The demand for the zones is also extracted from the same site. The operating limits of the generators used are as offered; however, the generator‘s parameters were artificially created (ramps, min-up/down times). We use the transmission network comprising 43 regions projected by Secretaría de Energía (2018). The parameters of reservoirs are created artificially, too. The data for this instance can be found in this repository: https://github.com/urieliram/DAM.

The elements modeled in the Central Interconnected System (CIS) power system are: Intervals: 24; thermal units: 255; hydroelectric units: 63; river basins: 8; renewable: 64; buses: 45; lines: 64; tie-lines: 64; loads: 6152; reservoirs: 16. The model has around 331,358 variables (298,768 are continuous and 32,590 are binary) and 240,080 constraints. The solution method scales really well as it has ben capable of solving instances of up to 100 renewable units and over 340,000 variables which are largest in the database.

Figure 2 shows the expected load demand of the instance and the energy price component or dual variables of the power balance constraints. The load demand varies from 30,000 to 38,000 MW while the prices vary from 1,000 \$/MW to 1,900 \$/MW. As shown in Figure 2, the prices follow the expected demand trend, so the higher the demand goes, the higher the prices get. Additionally, the renewable energy sources, represented by the cyan (wind) and yellow (solar) bars, correspond to parameters from the mathematical model and are derived from forecasting methods. These sources, encompassing approximately 14% of the total system demand, contribute significantly to the overall system dynamics, emphasizing the critical interplay between renewable generation and the prevailing load-demand conditions. As part of future work, we acknowledge the importance of addressing the uncertainty associated with these sources and their potential impact on the economic and security dynamics of the system.

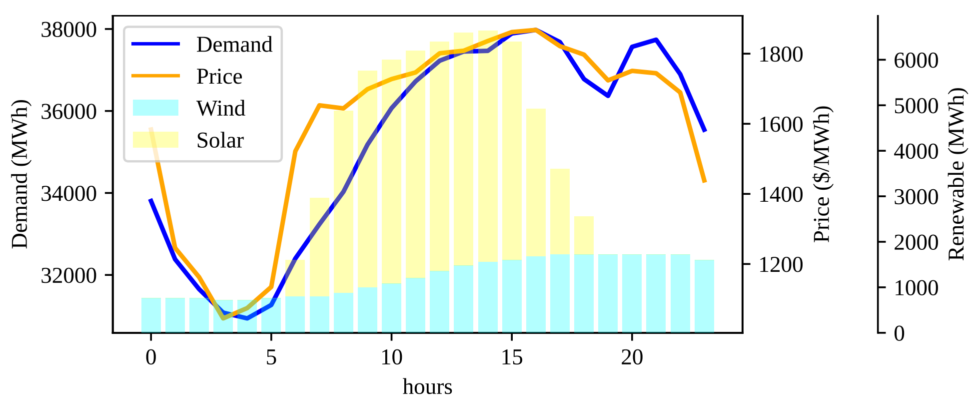

Figure 2: Expected load demand and energy prices.

Figure 3 shows that MP estimation of transmission losses matches SP calculation accuracy starting from the second iteration and improving with each subsequent one.

Figure 4 illustrates the representative reservoir’s net hydraulic head and corresponding water

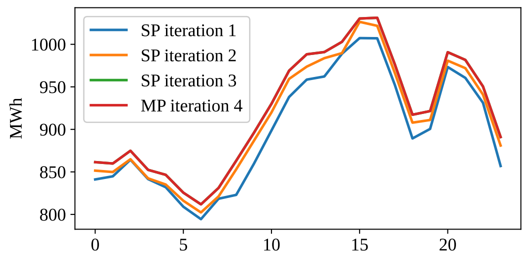

Figure 3: Transmission losses after the first iteration.

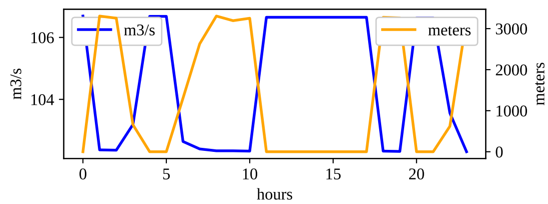

Figure 4: Net hydraulic head and water discharged.

discharge. It reveals that a hydroelectric unit's water requirement is inversely proportional to the reservoir's net hydraulic head, with higher heads requiring less water for energy production.

5.2 Experiment 2: Performance tests

This experiment aims to test the model's performance in other real-world instances using the CIS energy system of the electricity market in Mexico. The tests were carried out with four instance groups called MEM1, MEM2, MEM3, and MEM4. Each group has 80 instances made from publicly available information regarding the Wholesale Electricity Market (WEM) in Mexico. The original instances were modified by randomly choosing a percentage (70%, 80%, 90%, 95%) of all thermal generators, and the demand, reserve requirements and generator bids were modified. The number of instances for each percentage is 20. The dimensions of each of the instances are shown in Table 2. MEM1 and MEM2 represent typical summer days, whereas MEM3 and MEM4 represent typical winter days. The load demand of each group is shown in Figure 5.

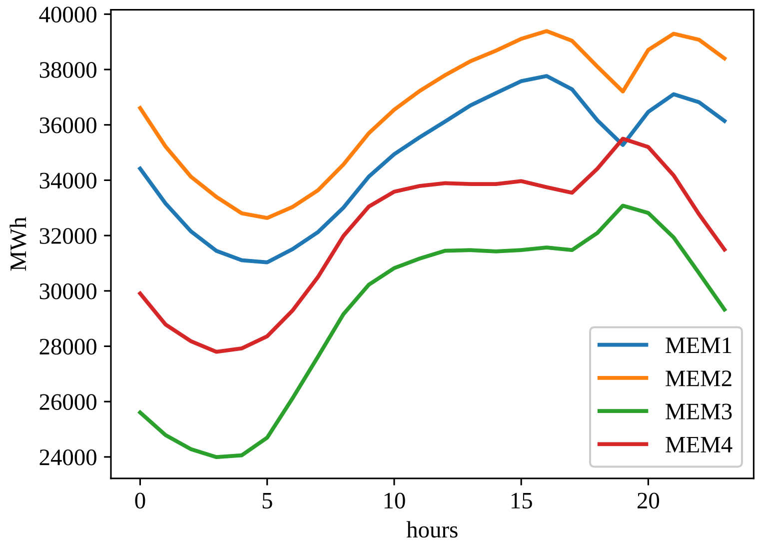

Figure 5: Summer and winter demands.

Table 2: Instance size by data set.

	MEM1 summer	MEM2 summer	MEM3 winter	MEM4 winter
Intervals	24	24	24	24
Thermal units	255	255	253	253
Hydroelectric units	63	63	63	63
Renewable units	64	64	74	74
River basins	8	8	8	8
Tie-lines	89	88	106	105
Reservoirs	16	16	16	16

The key variables to measure and analyze the performance of the model are: average CPU time ($\bar{t}$); worst CPU time ($\bar{t^*}$); the number of iterations (k) between the MP-subproblem (SP) until reaching the ($tolerance$); the number of cuts ($nviol$) added by the SP (one for each tie-line violated); recorded loss error estimation ($Errlosses$). The instances were solved using a relative optimality gap of 0.0001% and ($tolerance$) in the approximation losses tolerance of 0.005%. The problems are solved until they reach the time limit of 3500 seconds for each iteration or until they reach optimality. There is no time limit to solve the overall problem.

The results are outlined in Table 3. The column ($instances$) shows the names of each group of instances. The column ($\%$) indicates the percentage of thermal generators selected that can be committed for each group of instances. The columns ($\bar{t}$) and (t^*) the CPU average time and the CPU maximum time used to solve the instances are registered. The columns ($\bar{k}$) and (k^*) display the median and a maximum number of iterations between the MP and its SP for the

Table 3: Results for each instance.

instances		$\bar{t}$	t^*	$\bar{k}$	k^*	$\overline{nviol}$	$nviol^*$	$\overline{Errlosses}$	$\overline{profit}$
MEM1	70	8,593	24,573	3	5	17	25	0.0031	\$1,880,824,498
	80	8,948	23,455	3	5	16	19	0.0030	\$1,895,011,558
	90	14,375	29,437	3	4	17	20	0.0024	\$1,910,265,699
	95	14,755	46,101	3	4	16	19	0.0026	\$1,921,684,506
MEM2	70	4,829	20,534	3	4	9	12	0.0027	\$2,141,180,824
	80	6,494	19,403	3	5	10	12	0.0028	\$2,148,492,402
	90	6,362	19,112	3	3	10	12	0.0029	\$2,167,144,875
	95	7,484	20,734	3	5	9	11	0.0025	\$2,169,740,024
MEM3	70	4,632	18,493	5	7	14	19	0.0025	\$20,044,116,952
	80	6,234	12,001	6	6	16	21	0.0028	\$20,064,006,287
	90	9,779	22,156	6	8	13	19	0.0028	\$20,091,123,339
	95	11,075	20,344	6	8	12	15	0.0028	\$20,099,986,114
MEM4	70	1,952	5,107	4	7	8	13	0.0026	\$20,476,495,913
	80	3,060	7,173	4	5	6	9	0.0024	\$20,491,680,365
	90	9,873	26,767	4	7	7	9	0.0026	\$20,516,227,967
	95	15,147	37,117	5	5	8	9	0.0023	\$20,524,900,918

instances in each row. The column ($nviol$) records the median number of tie-lines violated in the SP that generated transmission cuts in the MP. The column ($\overline{Errlosses}$) captures the average approximation loss reached. The column ($profit$) marks the market's average economic profits. All instances reached the approximation losses tolerance required and the MILP gap by the MP's.

It is worth noting that the rough number of iterations k is between two and seven, yet it is assumed that this figure is related to a higher number of generators in the system. Likely, the transmission losses wane and wax depending on the number of generators connected in the system.

The average error in estimating transmission losses in all instances is less than 0.005%; for instance, it represents an error of 0.00268% in a setting with maximum losses of 105.36 MW.

To further analyze the impact of transmission losses on the power system, we present Figure 6 that displays and compares losses across summer and winter energy scenarios in Mexico. This figure shows the distribution of losses along seasonal differences. As can be seen from the figure, during the summer months, with peak demands reaching approximately 39,388 MW, average losses range from 713 MW to 994 MW, representing 1.8% to 2.8% of the maximum demand. In winter, when peak demand is closer to 35,500 MW, losses vary between 518 MW and 909 MW, accounting for 1.4% to 2.5% of the maximum demand. While the relative percentages are modest, the absolute magnitudes are substantial and must be considered when modeling operational costs and transmission efficiency.

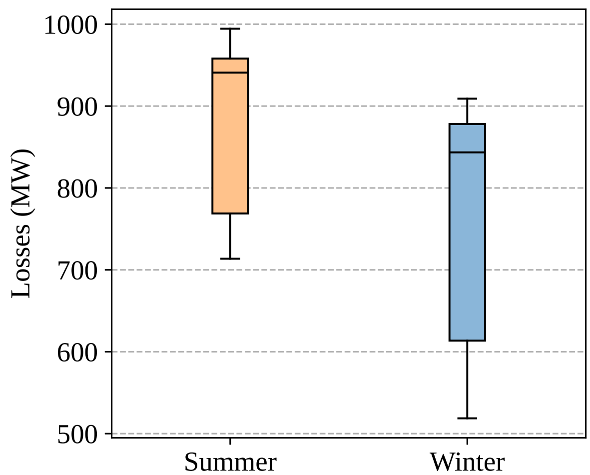

Figure 6: Hourly transmission losses in summer and winter scenarios.

An expected result is the increase of CPU time when the instances are solved due to a higher percentage of generators. This rise is produced by the increased combinatorial complexity of the UCP model. Another expected behavior is the decrease of profits with the rise in the generation offer caused by a higher number of generators in the system. This increment emulates an increasing competence in the market. With 95% of available generation, the economic profits nearly reach the minimum value.

Figures 7, 8, 9, and 10 have been designed to analyze the behavior of economic profits, CPU time, number of of iterations between MPs and SPs, and the number of family of transmission cuts added to the MP. On one hand, in the profit subfigure of Figures 7, 8, 9, and 10 the vertical axis represents the benefit of participant in millions of pesos. On the other hand, in the CPU time subfigure, the vertical axis represents processing time. The horizontal axis represents the percentage of thermal generators to be committed for all Figures. The boxes represent statistical results of 20 randomly generated instances for each percent (70%, 80%, 90%, 95%) for each group (MEM1, MEM2, MEM3, MEM4).

As it is observed in Table 2 and Figures 7, 8, 9, and 10, is shown a coherent behavior depicting a reduction of economic profits related with a higher number of generations in the system. Also, the results indicate that the more generators in the system, the more CPU time is required to process the data. It is shown that the economic benefits increase gradually with the increment of generators in the system since the instances resolved are closer to 100% of units. This pattern matches normal expectations. Furthermore, CPU times gradually increase while more generators are added to the system. This increase is an expected pattern since a more significant number of generators working entails more units to commit and a more complex problem to solve.

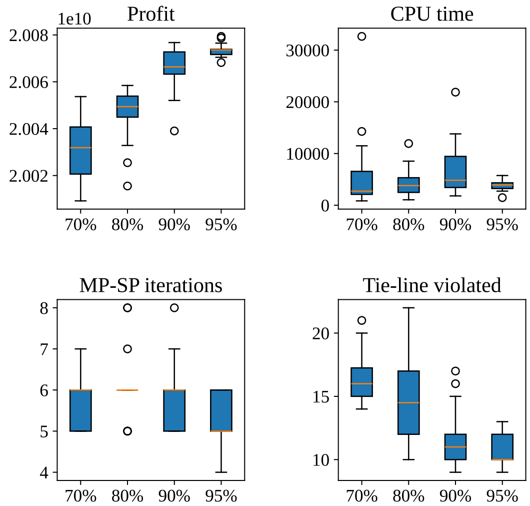

Figure 7: Results of MEM1 instances.

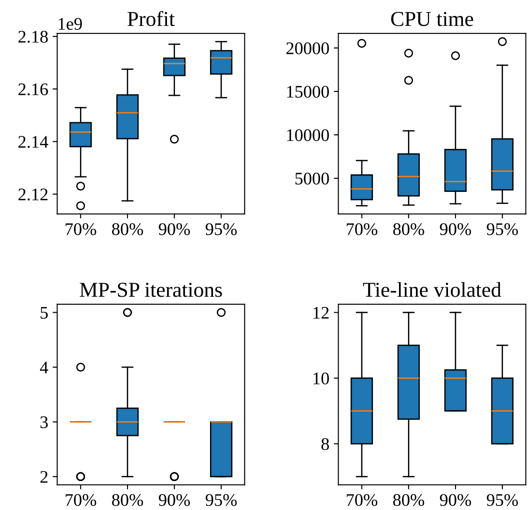

Figure 8: Results of MEM2 instances.

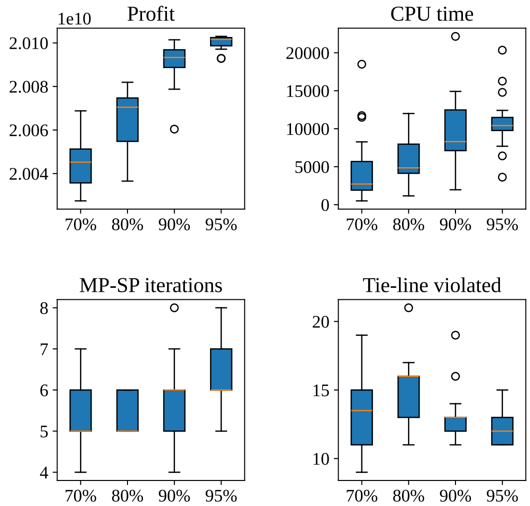

Figure 9: Results of MEM3 instances.

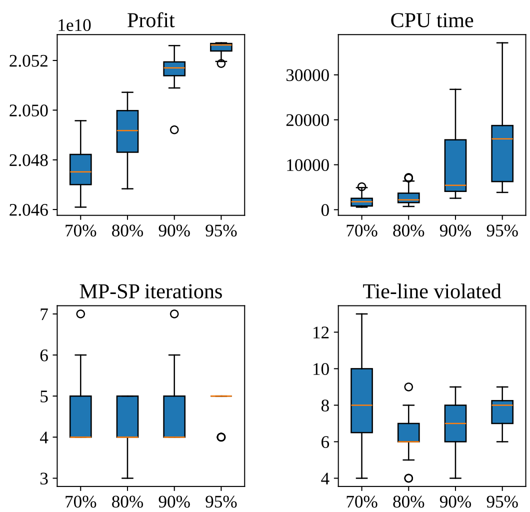

Figure 10: Results of MEM4 instances.

6 Conclusions

This work demonstrates that the model and its proposed method help determine the generators' production schedule in the day-ahead market. The model simultaneously optimizes energy and reserves and sets the maximum economic profit of the participants in such a market. The model consists of a large-scale mixed-integer non-linear programming (MINLP). To deal with its non-linear feature, several approximation methods were adopted to reduce it into a mixed-integer linear program (MILP). For instance, the hydropower function's non-linear feature was handled using the Taylor series polynomial. This approach is a simple but innovative solution to the problem of hydrothermal coordination.

Simulation results are presented on key representative instances of the wholesale electricity market in Mexico to demonstrate that the model is consistent and applicable to other markets that require hydrothermal coordination.

There are several lines for future research, including applying our linearization method for hydro coordination with renewable energy sources and batteries in a stochastic framework. Additionally, we aim to incorporate re-pumping in reservoir modeling. Its potential inclusion in reservoir operations could enhance our hydro modeling. In addition, while the unique features of this model make other methods not directly applicable to solving this model, there are algorithmic frameworks that have been used for similar models that may be worthwhile exploring. These, of course, have to be adapted to handle the particular features and exploit the specific properties of the proposed model. Finally, while in our work we used a linearization technique that is easy to implement, there are other traditional linearization methods such as the fourth-dimensional HPF linearization (Diniz and Maceira, 2008) and the McCormick's envelope technique (Castro, 2015; Bynum et al., 2018) that should be further analyzed. In this vein, it would be interesting to compare and analyze the trade-offs among these methods in terms of solution accuracy, computational time, and solution quality.

Acknowledgments: The presentaion of this work has been imporved thanks to the remarks of three anonymous reviewers and the editor. Uriel Lezama-Lope was supported by a scholarship for doctoral studies from the Mexican Council for Research and Technology (CONACyT), by UANL, and by INEEL. In addition, the authors thank CENACE for making the data available through its public website.

References

Abdi, H. (2021). Profit-based unit commitment problem: A review of models, methods, challenges, and future directions. *Renewable and Sustainable Energy Reviews*, 138:110504.

Álvarez López, J., Ceciliano-Meza, J. L., and Guillén Moya, I. (2015). The challenges of the unit commitment problem for real-life small-scale power systems. *International Journal of Electrical Power & Energy Systems*, 71(1):112–122.

Álvarez López, J., Ceciliano-Meza, J. L., Guillén Moya, I., and Nieva Gómez, R. (2012). A MIQCP formulation to solve the unit commitment problem for large-scale power systems. *International Journal of Electrical Power & Energy Systems*, 36(1):68–75.

Babona, N. and Rossell Pujós, F. (1999). Formulation of the short-term hydrothermal coordination of electricity generation and solutions through mixed integer programming. Technical Report DR 99/06, Universitat Politécnica de Catalunya, Barcelona, Spain.

Bisanovic, S., Hajro, M., and Dlajic, M. (2010). Mixed integer linear programming based thermal unit commitment problem in deregulated environment. *Journal of Electrical Systems*, 6(4):466–479.

Bisanovic, S., Hajro, M., and Dlakic, M. (2008). Hydrothermal self-scheduling problem in a day-ahead electricity market. *Electric Power Systems Research*, 78(9):1579–1596.

Bynum, M., Castillo, A., Watson, J.-P., and Laird, C. D. (2018). Strengthened SOCP relaxations for ACOPF with McCormick envelopes and bounds tightening. *Computer Aided Chemical Engineering*, 44:1555–1560.

Castillo, A., Laird, C., Silva-Monroy, C., Watson, J. P., and O'Neill, R. P. (2016). The unit commitment problem with AC optimal power flow constraints. *IEEE Transactions on Power Systems*, 31(6):4853–4866.

Castro, P. M. (2015). Tightening piecewise McCormick relaxations for bilinear problems. *Computers & Chemical Engineering*, 72:300–311.

Catalão, J. P. S., Pousinho, H. M. I., and Mendes, V. M. F. (2010). Scheduling of head-dependent cascaded hydro systems: Mixed-integer quadratic approach. *Energy Conversion and Management*, 51(3):524–530.

Ceciliano-Meza, J. L., de la Torre, A., Álvarez López, J., and Nieva Gómez, R. (2016). Formulación matemática del modelo de asignación de unidades con restricciones de seguridad y cálculo de precios marginales locales y de servicios conexos en el mercado de un día en adelanto. Technical Report 1.0, Centro Nacional de Control de la Energía, Mexico. Available at: https://www.cenace.gob.mx/Docs/MercadoOperacion/Formulación Matemática Modelo AU-MDA y PML v2016 Enero.pdf, in Spanish.

Chow, J. H., Mello, W. D., and Cheung, K. W. (2005). Electricity market design: An integrated approach to reliability assurance. *Proceedings of the IEEE*, 93(11):1956–1969.

Colonetti, B. and Finardi, E. C. (2020). Combining Lagrangian relaxation, Benders decomposition, and the level bundle method in the stochastic hydrothermal unit-commitment problem. *International Transactions on Electrical Energy Systems*, 30(9):e12514.

Conejo, A. J., Arroyo, J. M., Contreras, J., and Villamor, F. A. (2002). Self-scheduling of a hydro producer in a pool-based electricity market. *IEEE Transactions on Power Systems*, 17(4):1265–1272.

de Queiroz, A. R. (2016). Stochastic hydro-thermal scheduling optimization: An overview. *Renewable and Sustainable Energy Reviews*, 62:382–395.

Diniz, A. L. and Maceira, M. E. P. (2008). A four-dimensional model of hydro generation for the short-term hydrothermal dispatch problem considering head and spillage effects. *IEEE Transactions on Power Systems*, 23(3):1298–1308.

Diniz, A. L. and Souza, T. M. (2014). Short-term hydrothermal dispatch with river-level and routing constraints. *IEEE Transactions on Power Systems*, 29(5):2427–2435.

dos Santos, T. N. and Diniz, A. L. (2011). A dynamic piecewise linear model for DC transmission losses in optimal scheduling problems. *IEEE Transactions on Power Systems*, 26(2):508–519.

Ezzati, S. M., Yousefi, G. R., Pedram, M. M., and Baghdadi, M. (2010). Security-constrained unit commitment based on hybrid benders decomposition and mixed integer non-linear programming. In *IEEE International Energy Conference*, pages 233–237, Manama, Bahrain.

García Félix, G. (2017). *Análisis de modelos para la asignación de pérdidas en el cálculo del precio marginal local en el mercado eléctrico mayorista*. Master's thesis, Tecnológico de Monterrey, Monterrey, Mexico. In Spanish.

Geoffrion, A. M. (1970). Primal resource-directive approaches for optimizing non-linear decomposable systems. *Operations Research*, 18(3):375–403.

Gil, E., Bustos, J., and Rudnick, H. (2003). Short-term hydrothermal generation scheduling model using a genetic algorithm. *IEEE Transactions on Power Systems*, 18(4):1256–1264.

Guo, J., Zhang, J., Zhao, T., and Qi, X. (2024). Stochastic unit commitment for power systems with offshore wind farms towards frequency resiliency. *IET Renewable Power Generation*, 18(7):1218–1229.

Håberg, M. (2019). Fundamentals and recent developments in stochastic unit commitment. *International Journal of Electrical Power & Energy Systems*, 109:39–48.

Helseth, A., Melo, A. C. G., Ploussard, Q. M., Mo, B., Maceira, M. E. P., Botterud, A., and Voisin, N. (2023). Hydropower scheduling toolchains: Comparing experiences in Brazil, Norway, and USA and implications for synergistic research. *Journal of Water Resources Planning and Management*, 149(7):04023030.

Hinojosa, V. H. and Gutiérrez-Alcaraz, G. (2017). A computational comparison of 2 mathematical formulations to handle transmission network constraints in the unit commitment problem. *International Transactions on Electrical Energy Systems*, 27(8):e2332.

Kong, J., Skelbred, H. I., and Fosso, O. B. (2020). An overview on formulations and optimization methods for the unit-based short-term hydro scheduling problem. *Electric Power Systems Research*, 178:106027.

Kotharij, D. P. and Dhillon, S. (2010). *Power System Optimization*. PHI Learning, New Delhi, India, 2nd edition.

Kwon, K.-B. and Kim, D. (2020). Enhanced method for considering energy storage systems as ancillary service resources in stochastic unit commitment. *Energy*, 213:118675.

Lezama Lope, U. I. (2023). *Efficient Methods for Solving Power System Operation Scheduling Challenges: The Thermal Unit Commitment Problem with Staircase Cost and the Very Short-term Load Forecasting Problem*. Phd thesis, Universidad Autonoma de Nuevo Leon, San Nicolas de los Garza, Mexico.

Lima, R. M., Constante-Flores, G. E., Conejo, A. J., and Knio, O. M. (2024). An effective hybrid decomposition approach to solve the network-constrained stochastic unit commitment problem in large-scale power systems. *EURO Journal on Computational Optimization*, 12:100085.

Liu, X., Conejo, A. J., and Constante Flores, G. E. (2023). Stochastic unit commitment: Model reduction via learning. *Current Sustainable/Renewable Energy Reports*, 10:36–44.

Ma, X., Song, H., Hong, M., Wan, J., Chen, Y., and Zak, E. (2009). The security-constrained commitment and dispatch for Midwest ISO day-ahead co-optimized energy and ancillary service market. In *2009 IEEE Power Energy Society General Meeting*, pages 1–8, Calgary, Canada.

Marín-Cano, C. C., Sierra-Aguilar, J. E., López-Lezama, J. M., Jaramillo-Duque, A., and Villa-Acevedo, W. M. (2019). Implementation of user cuts and linear sensitivity factors to improve the computational performance of the security-constrained unit commitment problem. *Energies*, 12(7):53–72.

Mena, R., Godoy, M., Catalán, C., Viveros, P., and Zio, E. (2023). Multi-objective two-stage stochastic unit commitment model for wind-integrated power systems: A compromise programming approach. *International Journal of Electrical Power & Energy Systems*, 152:109214.

Menezes, T. V. and da Suva, L. C. P. (2006). A method for transmission loss allocation based on sensitivity theory. In *2006 IEEE Power Engineering Society General Meeting*, pages 1–6, Montreal, Canada.

Olivos, C. and Valenzuela, J. (2025). Stochastic unit commitment problem: A statistical approach. *Expert Systems with Applications*, 273:126787.

Pan, S., Jian, J., and Yang, L. (2022). Solution to dynamic economic dispatch with prohibited operating zones via MILP. *Mathematical Biosciences and Engineering*, 19(7):6455–6468.

Polimeni, S., Moretti, L., E, M., S, L., and Manzolini, G. (2023). A novel stochastic model for flexible unit commitment of off-grid microgrids. *Applied Energy*, 331:120228.

Santos, T. N., Diniz, A. L., Saboia, C. H., Cabral, R. N., and Cerqueira, L. F. (2020). Hourly pricing and day-ahead dispatch setting in Brazil: The DESSEM model. *Electric Power Systems Research*, 189:106709.

Secretaría de Energía (2018). Programa de desarrollo del sistema eléctrico nacional 2018-2032. Report, available at: https://base.energia.gob.mx/prodesen/PRODESEN2018/PRODESEN18.pdf. In Spanish.

Šepetanc, K. and Pandžić, H. (2020). Convex polar second-order Taylor approximation of AC power flows: A unit commitment study. *IEEE Transactions on Power Systems*, 36(4):3585–3594.

Shang, C., Li, L., Ge, Y., Zhai, S., Song, X., Cao, Q., and Ai, Q. (2024). Robust planning upon unit commitment. *International Journal of Electrical Power & Energy Systems*, 157:109890.

Taktak, R. and D'Ambrosio, C. (2016). An overview on mathematical programming approaches for the deterministic unit commitment problem in hydro valleys. *Energy Systems*, 8:57–79.

Yu, Z., Sparrow, F. T., Bowen, B., and Smardo, F. J. (2000). On convexity issues of short-term hydrothermal scheduling. *International Journal of Electrical Power & Energy Systems*, 22(6):451–457.